J Musculoskelet Neuronal Interact 2013; 13(3):353-367

Original Article

Hylonome

A long-term *in vivo* investigation on the effects of xenogenous based, electrospun, collagen implants on the healing of experimentally-induced large tendon defects

A. Oryan[1], A. Moshiri[2], A. Meimandi Parizi[2], I.A. Silver[3]

[1]Department of Pathology, School of Veterinary Medicine, Shiraz University, Shiraz, Iran; [2]Division of Surgery, Department of Clinical Sciences, School of Veterinary Medicine, Shiraz University, Shiraz, Iran; [3]Center for Comparative and Clinical Anatomy, School of Veterinary Science, South well Street, Bristol BS2 8EJ, UK

Abstract

Aim: This study was designed to investigate the effect of novel 3-dimensional (3-D) collagen implants on the healing of large, experimentally-induced, tendon-defects in rabbits. **Methods:** Forty mature male white New Zealand rabbits were divided randomly into treated and control groups. Two cm of the left Achilles tendon was excised and the gap was spanned by Kessler suture. In the treated group, a novel 3-D collagen implant was inserted between the cut ends of the tendon. No implant was used in the control group. During the course of the experiment the bioelectrical characteristics of the healing and normal tendons of both groups were investigated weekly. At 120 days post injury (DPI), the tendons were dissected and inspected for gross pathology, examined by transmission and scanning electron microscopy, and their biomechanical properties, percentage dry matter and hydroxyproline concentration assessed. **Results:** The collagen implant significantly improved the bioelectrical characteristics, gross appearance and tissue alignment of the healed, treated tendons, compared to the healed, control scars. It also significantly increased fibrillogenesis, diameter and density of the collagen fibrils, dry matter content, hydroxyproline concentration, maximum load, stiffness, stress and modulus of elasticity of the treated tendons, as compared to the control tendons. Treatment also significantly decreased peri-tendinous adhesions, and improved the hierarchical organization of the tendon from the collagen fibril to fibre-bundle level. 3-D xenogeneic-based collagen implants induced newly regenerated tissue that was ultrastructurally and biomechanically superior to tissue that was regenerated by natural unassisted healing. **Conclusion:** This type of bioimplant was biocompatible, biodegradable and appeared suitable for clinical use.

Keywords: Tendon, Healing, Implant, Collagen, Biomechanics, Ultrastructure

Introduction

Tendon defects are one of the most common and disabling acute orthopedic disorders[1]. Several techniques are used to restore the mobility of patients but all have significant limitations[2]. Tendon auto or allo transplantation is currently the method of choice but has major limitations associated with donor site morbidity, availability, cost, biohazards, infections, and ethical concerns[3-6]. Tissue engineering has also provided useful outcomes in both human and animal patients[4,5]. Currently the most available tissue-engineered graft is a de-cellularized xenogeneic-based collagen scaffold, derived from animal tissue[7-9]. The most critical processing stage in preparation of these scaffolds is de-cellularization of the graft[10,11]. Despite the often beneficial effects of these products, inability of the manufacturers either to align the nano or microstructure of the collagen or delete all non-collagenous elements such as glycosaminoglycans, enzymes and other tissue constituents, is a major limitation of such prostheses[4,12]. Removing the non-collagenous materials in the tissue increases the biocompatibility of the scaffold which reduces rejection and enhances incorporative behavior of the scaffold with the healing tissue[4,7,8]. Complete removal of cells and non-collagenous elements by tissue processing is extremely difficult because of their adherence to the collagen fibres[4,10,13].

The authors have no conflict of interest.

Corresponding author: Dr Ali Moshiri, DVM. DVSc, (Veterinary Surgery)
E-mail: dr.ali.moshiri@gmail.com

Edited by: S. Warden
Accepted 5 June 2013

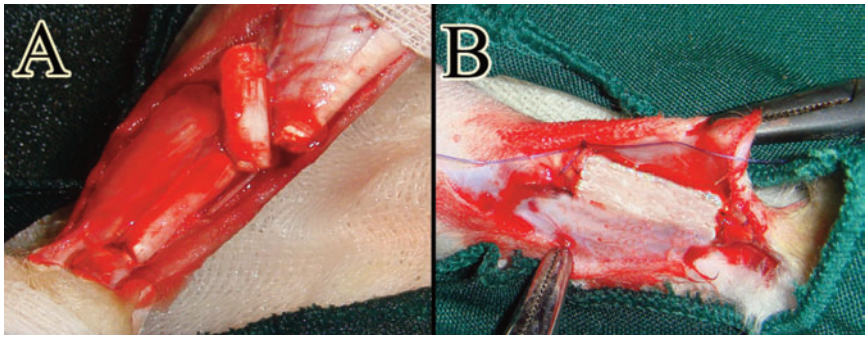

Figure 1. (**A**) Two cm of the left Achilles tendon of the rabbit was excised. (**B**) The collagen implant was inserted into the injured area and modified Kessler core pattern was used to maintain a two cm gap and secure the collagen implant.

Electrospinning is a newer approach to synthesising two- or three-dimensional tissue-engineered scaffolds[14-16]. By this technology, fibres are produced in uni-directional, parallel alignment. *In vitro* investigations have demonstrated that this characteristic enhances cell migration and differentiation[11,16]. The major limitations of the technology are availability of the electrospinning devices, weak biomechanical properties of the collagen-based constructs and perhaps cost, especially in respect of three-dimensional structures[17,18]. Currently, electrospinning is used for making engineered products for surgical reconstruction of vascular defects[14,16].

Collagen gel technology for constructing 3-dimensional scaffolds used for the culture of stem cells[19], has the major limitation for application to tendon repair in that its randomly-organized polymerized collagen fibres encourage migrating cells to proliferate in more than one direction and therefore tend to initiate peritendinous adhesion[20,21].

For all methods described to date, collagen is the most important component used to construct 2- or 3-dimensional scaffolds[14,15,22]. Not only is it chemo-attractive with a role in increasing cell migration and proliferation, but also possesses the essential characteristic of biocompatibility, and is readily available[10,19,23,24].

Ideal grafts for reconstructive tendon surgery are those that are easily available, biocompatible, biodegradable, and with highly aligned structural elements that attract unidirectional migration of proliferating cells[4,5]. Currently there are no generally well-accepted and approved tissue-engineered grafts for reconstructive tendon surgery[4,25], possibly because most investigations of potential graft prostheses have focused on their *in vitro* behavior[4,12,19]. Such investigations do not address how well the scaffolds tolerate the immune and cellular responses of the host towards them[4]. Theoretically, it might be expected that the xenogeneic-based, non-self-collagen should be rejected after implantation in a host, but this cannot be examined with *in vitro* studies[8,24].

It therefore seemed logical to produce a 3-dimensional collagen implant made with the electrospinning technology combined with components derived from gel technology. The authors used electrospinning to produce a highly aligned 2-D collagen scaffold. This scaffold was then used as a core during the polymerization process, to align unorganized collagen molecules produced in the gel system. By this processes the limitations of above methods were resolved and a novel 3-dimensional collagen implant was constructed. This was used as a prosthesis to reconstruct large, experimentally-induced tendon defect in rabbits. We hypothesized that continuity of the collagen implant would probably increase the rate of healing and that its highly oriented structure would encourage alignment of newly regenerated collagen fibrils and fibres. It was anticipated that the biomechanical properties of the newly regenerated tendinous tissue would probably be superior to those of tendon lesions that had been repaired by unassisted natural healing. Moreover, these collagen implants may have a role in increasing the length of the inflammatory response because they take longer to be absorbed. However at 120 DPI, the bioelectrical characteristics of the healing treated tendons should be closer to the normal values, obtained before surgery, than the healing control tendons.

Materials and methods

Study design

Forty skeletally-mature male White New Zealand rabbits of approximately 12 to 14 months age and 3.15±0.15 kg body weight were divided randomly into a treated (*n=20*) and control (*n=20*) groups. The left Achilles tendon of each animal in both groups was designated as the injured tendon (*n=20* tendons in each group) and the right (normal contra-lateral tendon (NCT)) tendon was left intact (*n=20* tendons in each group). The rabbits were housed in individual standard rabbit cages and maintained on standard pelleted rabbit diet with no limitation of access to food or water. The left Achilles tendon (Injured Treated Tendon (ITT)) of the treated group was compared with their right NCT and with the Injured Control Tendons (ICTs), at 120 Days Post Injury (DPI)[26,27].

Preparation of the collagen implant

Inner part of a bovine Achilles tendon was treated with 0.1% per acetic acid and rinsed in hypotonic saline to lyse all the re-

maining cells before extraction of the collagen molecules[28]. Type I collagen was extracted from the tendon using the standardized manufacturing method of Opocrin SpA described by Foltran et al.[15]. Type 1 collagen molecules were electrospun by an electrospinning device. Purification was checked using SDS-Page. Collagen molecules showed high molecular weight bands for a1 (I) and a2 (I) dimers and, at lower molecular weight, the typical bands of a1 (I) and a2 (I) chains of type I collagen.

A novel modification of the method was used by the authors to produce micro-structured combined with nanostructured collagen fibres. In this technique, we designed a stainless steel box (10 cm height, 10 cm width, and 10 cm length), temporarily divided horizontally by the ground collector plate into two equal sections. Collagen fibres were produced by electrospinning with the ground collector negative, and accumulated in the upper section, after which, a primary solution of collagen, as described above but with a concentration of 10% (w/v)[29], was added via a syringe needle to the top and bottom sections (above and below the ground collector). The ground collector was removed by sliding it through a slit in the side of the box without disturbing the electrospun collagen sheet. The lid of the box was closed and the box placed in an incubator at 37ºC for 2 hours to increase the homogeneity and polymerization of the solution[30]. To complete the polymerization stage and harden the cube of collagen fibres, the box was then cooled to 4ºC for 24 hours[29,31].

The cube of collagen was then removed from the box. The electrospun collagen matrix had acted as a core with oriented fibre characteristics and had caused alignment of newly-formed collagen fibres with diameters between 1.82±0.15 µm and 3.19±0.84 µm (mean measured for 100 fibres) in the gel system around its electrospun collagen fibres (diameters 100-600 nm)[20,32]. The hardened collagen gel was cut into several pieces of the same size and shape as rabbits' Achilles tendons (L=2 cm, H=3.5 mm, W=3 mm). They were then freeze-dried. These collagen implants were cross-linked by the method of Teng et al.[17]. To increase the linkage, implants were treated with 2% riboflavin solution followed by ultraviolet irradiation (UV) according to the method used for cross-linking corneal collagen in previous studies[33,34]. The final product was immersed in 0.9% saline to remove any residual enzymes and chemical reagents, and then freeze-dried. The prosthesis was finally sterilized with UV irradiation and ethanol (70%).

Premedication and anesthesia

Premedication was provided by intra-muscular injection of 1 mg/kg acepromazine maleate (Neuotranq 1%, Alfasan Co. Woerden, Netherlands) and the animals were anesthetized by intra muscular injection of 15 mg/kg Ketamine (Ketamin 10%, Alfasan Co. Woerden, Netherlands) combined with 0.05 mg/kg Xylazin hydrochloride (Xylasin 2%, Alfasan Co. Woerden, Netherlands)[1,35,36].

Injury induction and surgical reconstruction

The left hind limb of the animals was prepared according to the basic principles of aseptic surgery[35]. After longitudinal skin incision over its dorsal aspect, 2 cm of the Achilles tendon with the covering epitenon were excised by transverse incisions (Figure 1A), approximately 5 mm distal to the gastrocnemius muscle and 5 mm proximal to the calcaneal tuberosity. Primary reconstruction of the tendon extremities were conducted using double strand modified Kessler core pattern, by monofilament absorbable Polydioxanon suture material no 0-4 and a straight taper-cut orthopedic needle (PDS, Ethicon, INC.1997, *Johnson & Johnson*, USA). This aligned the remaining Achilles tendon extremities in a normal anatomical position and created a 2 cm gap between the extremities[1]. The same method was applied to both groups. For insertion of the prosthetic implant into the gap in the tendon the double strand suture was passed through the longitudinal axis of the implant (Figure 1B). The skin over the lesion was closed routinely.

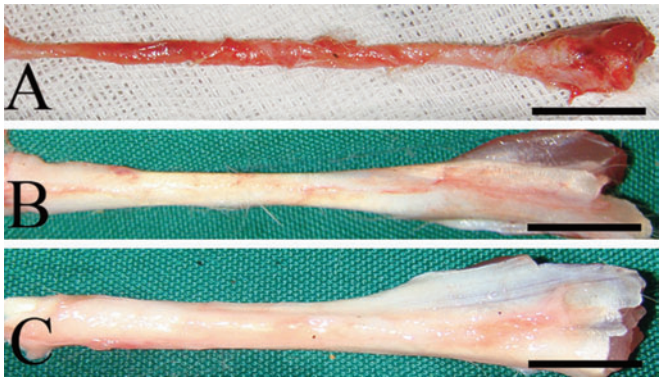

Figure 2. Gross appearance of the injured control tendon (**A**) injured treated tendon (**B**) and intact tendon (**C**) at 120 DPI. (**A**) The injured control tendon shows hyperemia and the gastrocnemius muscle is severely atrophic. The proximal and distal parts of the original tendon have degenerated and are unrecognisable, being covered by newly regenerated tissue which fills the injury. The gross appearance of this repair resembles loose areolar connective tissue. (B) In the treated injury the collagen implant has been completely absorbed and replaced by newly regenerated homogenous tendinous tissue between gastrocnemius and calcaneal tuberosity. No muscle atrophy is seen. There is no hyperemia and the transverse diameter of this tendon is similar to that of normal tendons. Scale bar=1 cm.

Bioelectrical characteristics

The direct transmission electrical current (DTEC; micro-amp) and the tissue resistance to direct electrical current (TRDEC; micro-ohm) of the ITTCs, ICTs and their NCTs, were measured with a digital multi pen type meter (Mastech Seoul, South Korea). The negative probe was placed on the skin on the medial side and the positive probe on the skin on the lateral side of the Achilles tendon. DTEC and TRDEC were recorded at weekly intervals from days 0 to 120 post injury.

The bioelectrical characteristics of the injured tissues undergo specific changes during different phases of tendon heal-

Gross pathological findings (visual observation)			
Score	**Peritendinous adhesion**	**Hyperemia**	**Status**
0	No adhesion.	No hyperemia, shiny glistening surface appearance.	Normal
1	Tendon was easily detached from surrounding tissues by blunt dissection.	Occurred only in the paratenon.	mild
2	Detachment of tendon from surrounding tissues required a little sharp dissection.	It has extended to the tendon proper but it is not severe.	Moderate
3	Detachment of tendon from surrounding tissues required extensive sharp dissection.	It extendswidely into the tendon proper making its colour more pink and dark.	Severe
Score	**General appearance**	**Muscle Atrophy**	**Status**
0	The tendon is a discrete, homogenous structure of constant diameter clearly differentiated from the surrounding tissue and continuous between the gastrocnemius muscle and calcaneal tuberosity.	The transverse diameter of the largest bulk of the muscle is more than or equal to 350 % of the transverse diameter of the largest part of the Achilles tendon at its mid part.	Normal
1	As above but the diameter of the injured area is greater than the proximal and distal parts of the tendon. The tendon generally is a discrete structure.	The transverse diameter of the largest bulk of the muscle is more than or equal to 250 % of the transverse diameter of the largest part of the Achilles tendon at its mid part.	Mild
2	As above but the diameter of the injured area is less than that of the proximal and distal parts of the tendon. The tendon generally is a discrete structure.	The transverse diameter of the largest bulk of the muscle is more than or equal to 200 % of the transverse diameter of the largest part of the Achilles tendon at its mid part.	Fairly moderate
3	The injured area of the tendon is not a clearly defined collagenous structure but the proximal and distal parts are.	The transverse diameter of the largest bulk of the muscle is more than or equal to 150 % of the transverse diameter of the largest part of the Achilles tendon at its mid part.	Moderate
4	The whole tendon is not a clearly defined structure. No recognisable tendon is seen between the gastrocnemius muscle and calcaneal tuberosity but the *tibialis posterior* tendons is visible. Normally the Achilles tendon covers the *tibialis posterior* muscle but here, due to lysis of the Achilles tendon, the muscle is exposed.	The transverse diameter of the largest bulk of the muscle is more than or equal to 100 % of the transverse diameter of the largest part of the Achilles tendon at its mid part.	Severe
Score	**Muscle fibrosis**		**Status**
0	No fibrosis is seen in the gastrocnemius muscle and the tendinous portion of the Achilles is the only connective tissue that covers the muscle.		Normal
1	Mild fibrosis is seen in the muscle but more than 75% of the muscle is red color and has the gross appearance of muscle.		Mild
2	Between 50 and 74% of the gastrocnemius has the characteristics of muscle but fibrosis is obvious.		Moderate
3	More than 50% of the muscle shows fibrosis and the fibrous tissue fills the spaces between muscle fibers.		Severe
4	No characteristic muscular tissue can be seen in the gastrocnemius because all of it has been replaced by fibrous tissue.		Extremely severe

Table 1. Base scoring system used for defining the gross pathological findings.

ing. After tendon injury, hydration and wet weight of the injured area is enhanced as the inflammation and edema are elevated. At initial stages of the healing process, the TRDEC decreases and more electrical ions could be transferred through the injured area; thus, the DTEC increases. During the fibroplasia and remodeling phases of tendon healing, there is elevation in the collagen content, dry matter content, collagen alignment and tissue organization, and on the other hand there is reduction in the tissue hydration, inflammation and edema and these changes result in TRDEC elevation. Thus lower electrical ions could be transferred through the remodeled tissue and the DTEC decreases. Measurement of DTEC is an index of tissue hydration, edema and inflammation and measurement of TRDEC is an index of collagen quality and quantity, dry matter content and tissue remodeling[1,37].

PDGF level

Platelet Derived Growth Factor (PDGF) causes cell migration and proliferation. It also acts as chemo-attractant for monocytes, fibroblasts and neutrophils. PDGF increases synthesis of collagen and regulates angiogenesis. PDGF is produced shortly after tendon injury and stimulates production of other growth factors. After tendon injury the serum PDGF level increases and as the healing response is stronger, the serum PDGF level is higher. Therefore elevation of PDGF level is one of the indicators for the quality of tendon healing. This method is a non-invasive method which has strong clinical relevance[38].

Immediately before euthanasia, 10 ml blood was collected from each animal. Blood samples were placed in a regular tube (without EDTA) and centrifuged for 10 minutes to collect the serum. Serum PDGF concentration was measured with a com-

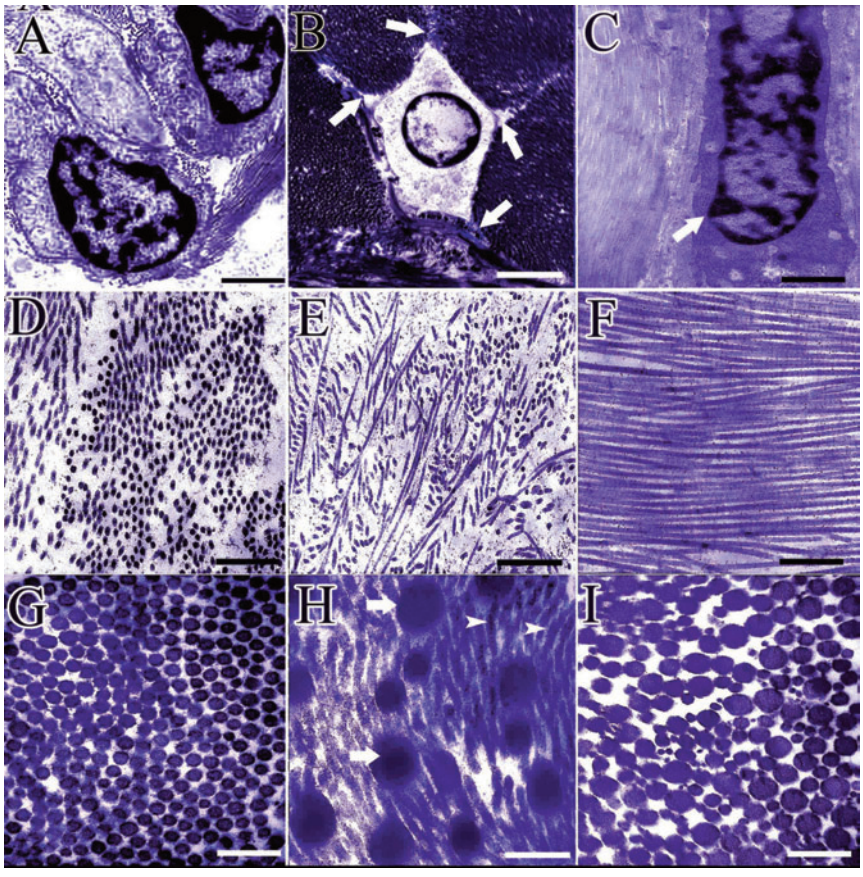

Figure 3. Transmission Electron Microscopy. (**A**) Immature tenoblasts. They are newly differentiated and are metabolically active. They are not elongated and are circular (scale bar, SB=2943 nm). The proportion of the nucleus/cytoplasm is low. (**B**) Transverse section of a mature tenocyte. They contain large numbers of elaborate extensions (arrows), and also junctions with one another. The nucleus/cytoplasm is higher than that in the tenoblast (**A**) (SB=2271 nm). (**C**) Tenocyte (arrow) (SB=1226 nm). This cell is cigar-shaped with less cytoplasm than tenoblasts. Metabolic activity is also lower than in tenoblasts. Note newly regenerated collagen fibrils aligned along the long axis of this cell. (**D**) (SB=570 nm) and (**E**) (SB=743 nm): injured control tendons. The transverse diameters of these newly regenerated collagen fibrils are small and they are immature. They are randomly oriented and are seen in both transverse and longitudinal aspects in the same field. (**E**) Collagen fibril density is very low; no fibrillar differentiation is visible. All fibrils are small-sized and uniform. (**F**) Longitudinal orientation of closely-packed collagen fibrils of injured, treated tendons. These fibrils are all newly synthesised (SB=395 nm). (**G**) Transverse section of regenerated collagen fibrils in the injured, treated tendon. These fibrils are more mature and have larger diameters compared to those of untreated controls. They are bimodal, aligned unidirectionally and are compact (SB=492 nm). (**H**) Two different collagen fibrils in the injured, treated tendons (SB=629 nm). Arrow-heads indicate newly regenerated collagen fibrils, while arrows show preserved collagen fibrils of the prosthesis. Note the difference between the diameters of these two types of collagen fibrils. Those of the newly regenerated fibrils are less than 100 nm but those of the old collagen fibrils of the collagen implant are more than 500 nm. The newly regenerated fibrils are aligned in parallel with the collagen fibrils of the prosthesis and it appears that the collagen implant fibrils act as a scaffold for these newly fibrils. (**I**) The intact tendon (SB=629 nm). Collagen fibrils are distributed in one direction and are all transversely sectioned. They are multimodal and more than 5 different diameters of the collagen fibrils are seen. The largest diameter collagen fibrils in the intact tendon are less than 307 nm which is smaller than the fibrils of the collagen implant.

mercial ELISA kit: Platelet-Derived Growth Factor AA (PDGF-AA) and AB Immunoassay (Biotrend Chemicals, LLC136 South Holiday Road, Unit C, Destin, FL 32550) according to the methods of Czarkowska-paczek et al.[38].

Ethics and euthanasia

The investigators who undertook the clinical observations, measurements and analysis of results in the present study were unaware of the experimental design and grouping details. All animals received humane care in compliance with the Guide for Care and use of Laboratory Animals published by the National Institutes of Health (NIH publication No. 85-23, revised 1985).

All operative procedures were performed by one surgeon. Postoperative analgesia with fentanyl (Matrifen, Roskilde, DK; 0.0015 mg/kg/h) was provided for 3 days via a transdermal patch applied to the depilated and sutured skin. Due to strict aseptic surgery and the sterility of the implant, no antibiosis was used and no wounds became infected.

The animals were euthanatized by intra-cardiac injection of a combination of 1 mg/kg gallamine triethiodide (Specia Co.

Paris, France), 15 mg/kg Ketamine (Ketamin 10%, Alfasan Co. Woerden, Netherlands), 2 mg/kg Xylasin (Xylazin 2%, Alfasan Co. Woerden, Netherlands), and 1 mg/kg Acepromazine maleate (Acepromazin 1%, Neurotranq, Alfasan Co. Woerden, Netherlands). The study was approved by the local ethical committee of our faculty.

Sample collection

Each injured tendon and its contralateral control was dissected and assessed for gross pathology (*n=20* left and *n=20* right for each group). The samples from each group were randomly divided into two equal subgroups. Subgroup 1 was used for biomechanical testing and subgroup 2 for biochemical and ultrastructural analysis. The tendons in subgroup 2 were divided longitudinally into two parts. Part A was used for determination of hydroxyproline and dry matter content and part B for transmission and scanning electron microscopy[39-41].

Gross pathology

Each injured tendon (*n=20* for each group) or NCT (*n=20* for each group) was evaluated for color changes, adhesion to the surrounding tissues and any other abnormalities. Each tendon was photographed and the images transferred to computer software (Adobe Photoshop CS-5 Extended, Ca, USA) and analyzed by computerized morphometry. Hyperemia, peritendinous adhesions, general appearance, muscle atrophy and fibrosis and tendon diameter were then measured and scored using the methods of Moshiri and Oryan[1], Oryan and Moshiri[35,36,42] (Table 1).

Transmission electron microscopy (TEM)

The method has been previously described[36]. Briefly, the samples were fixed in cold 4% glutaraldehyde, dehydrated in graded ethanol and embedded in epoxy resin 811 (TAAB, CO. London. UK). Transverse sections of 70-80 nm thickness were prepared and standard methods employed for production of the ultramicrographs (number of tendon samples in each group=10 left, 10 right, number of ultrathin sections in each tendon=5, number of ultramicrographs in each ultrathin section=5, totally 250 ultramicrographs for the left tendons and 250 ultramicrographs for the right tendons in each group). Number of collagen fibrils and elastic fibres were counted in all the ultramicrographs (magnification × 39000) and the results were expressed as mean and standard deviation (SD). The transverse diameter of all the collagen fibrils of all the ultramicrographs and the transverse diameter of one hundred elastic fibres were measured and the results were expressed as mean and SD. For the density of the collagen fibrils, the area (nm^2) of the collagen fibrils in the ultramicrographs were measured and reported as percentage of the total area (area of the ultramicrographs). The morphometric measurements were performed, using morphometric software (Image J, NIH, CA, USA and Adobe Co. Photoshop CS 5 extended. NY, USA). The mesenchymal cells were divided into tenoblasts (Figure 3A) and tenocytes (Figures 3B and 3C) based on the criteria which were provided in Table 2. In each group one hundred cells were counted and the number of tenocytes was reported as percentage of total mesenchymal cells. Alignment and maturity of the collagen fibrils and elastic fibres were scored and analyzed according to the criteria described in Table 2[36].

Scanning electron microscopy

The samples were gold-coated on a Copper mount. The surface and nano cross-section (thickness of each section=50 nm) and morphologies of collagen implants (*n=30*) were examined by scanning electron microscopy (SEM; Cambridge, London, UK). Magnifications from ×50 to ×30,000 were used to observe the morphological and morphometrical characteristics of the implants and tissue samples (*n=10 for left, n=10 for right*) (Table 2).

Hydroxyproline

The hydroxyproline concentration was measured spectrophotometrically by the methods of Dowling et al.[42] and Reddy[43]. Samples from the mid-lesion area of the injured and equivalent region of normal tendons of each animal of the treated and control groups were collected at 120 DPI and their hydroxyproline concentration was measured. The samples were hydrolyzed in 6 molar HCl at 105°C for 14-16 hr and hydroxyproline was oxidized by chloramine T and then a chromophore was formed by adding Ehrlich's reagent and incubating at 60°C. Interfering chromophores were removed by extracting them from the hydroxyproline product with toluene first in alkaline and then in acid media. The absorbance of the acid phase was read spectro-scopically at 543 nm and hydroxyproline content was calculated from a calibration curve based on standard solutions run in parallel with the samples.

Dry matter

For percentage dry weight analysis, the ITT, ICT and their NCT were weighed immediately after euthanasia, and then freeze-dried (Helosicc, Ink, Co. London, UK) until a constant weight was obtained and the percentage dry weight was then calculated according to the methods of Oryan et al.[35] and Moshiri and Oryan[1].

Biomechanical testing

The method has previously been described[35,41]. Briefly; the distal end of the Achilles tendons together with a portion of calcaneus were detached from the tars distally and 3 cm of gastroc-soleus muscle belly with its Achilles insertion were incised proximally. The tendons were vertically mounted onto a materials testing system (Instron® Tensile Testing Machine, London, UK). We used a dual-cryogenic fixation assembly, which held the tendon securely at both ends.

The gastroc-soleus muscle and the tendinous insertion over the muscle were clamped in the upper jaw and the distal part of the tendon including tendon and the calcaneal part were clamped in the distal jaw. The flow of liquid nitrogen through a chamber within the cryoclamp was used to freeze the tendon in the clamp to prevent slippage of the tendons. Up to 1 mil-

Alignment			
Score	**Description**	**Alignment of the collagen fibrils**	**Orientation of the fibroblasts and fibrocytes**
0	Near normal	Most are aligned in one direction.	Most lie along the long axis of collagen fibrils.
1	Highly aligned	More than 75% of the fibrils are aligned in one direction.	More than 75% of the cells lie parallel to collagen fibrils.
2	Moderately aligned	More than 50% of the fibrils are aligned in one direction.	More than 50% of cells lie along the direction of the collagen fibrils.
3	Fairly aligned	More than 25% of the collagen fibrils are aligned in one direction.	More than 25% of the cells lie in the direction of collagen fibrils.
4	Amorphous	Collagen fibrils are randomly oriented in no particular direction.	Most cells are not oriented in the direction of the collagen fibrils.
Description of the cells			
Cell name	**Morphological Description**		
Tenoblast	Cells with abundant cytoplasm in which there are many granules. The cells are metabolically active with collagen fibrils present in cytoplasmic vacuoles. The nuclei are pale and the width of the cells is more than 1100 nm. The ratio of cytoplasm/nucleus is high.		
Tenocytes	Cigar-shaped cells with dense nuclei. The ratio of cytoplasm/nucleus is low. The cell is not obviously metabolically active and the number of cytoplasmic granules is small.		
Maturity of the collagen fibrils in tendon			
Score	**Status**	**Description**	
0	Normal	Collagen fibrils are distributed in a multimodal pattern with a minimum of five different categories of fibril diameters, extremely small (0-64 nm), small (65-102 nm), medium (103-153 nm), large (154-256 nm) and extremely large (257-307 nm) visible in ultra-micrographs.	
1	Highly matured	Collagen fibrils are distributed in a multimodal pattern. Four different categories of fibril diameter, extremely small (0-64 nm), small (65-102 nm), medium (103-153 nm) and large (154-256 nm) are visible in ultra-micrographs.	
2	Matured	Collagen fibrils are distributed in a multimodal pattern. Three categories of fibril with diameters that are a) extremely small (0-64 nm), b) small (65-102) and c) medium (103-153 nm) are identifiable in ultra-micrographs.	
3	Immature	Collagen fibrils are distributed in a bimodal pattern. Two different categories of fibril diameter are a) extremely small (0-64 nm) and b) small (65-102 nm) and visible in ultra-micrographs.	
4	Highly immature	Collagen fibrils are distributed in a unimodal pattern. Only one category of fibril, extremely small (0-64 nm) is present in ultra-micrographs.	
Maturity of the elastic fibers			
Score	**Status**	**Description**	
0	Normal	The amorphous substance covered more than 90% of the elastic fibers	
1	Highly mature	The amorphous substance covered 50-90% of elastic fibers	
2	Fairly mature	The amorphous substance covered 25-50% of elastic fibers	
3	Immature	The amorphous substance covered 0-25% of elastic fibers	

Table 2. Base scoring criteria used for defining the differences between the ultra-structural characteristics of the injured treated and injured control tendons.

limeter of the tendon samples beyond the jaws were frozen. The freezing technology did not have any deleterious effect on the tensile testing results.

A 30 millimeter portion of the tendon sample was adjusted between the jaws. Petroleum jelly was applied to the tested portions of the tendons to prevent dehydration and thermal injury. A heater was centered to prevent freezing of the portion to be tested, and two cardboard insulators protected the ice surface from melting. This setup ensured a sharp temperature gradient between the frozen ends of the tendon and the portion to be tested, which was done at rabbit body temperature (37°C). Temperature of the portion to be tested was measured by a laser heat detector device (A real time temperature recorder) prior and during tensile testing. Two thermocouples (one in each cryofixation assembly) closely monitored the degree of freezing. Care was taken to use the same condition for all the samples including treatment, control and intact tendons.

Each tendon was loaded by elongating it at a displacement rate of 10 $mm \cdot s^{-1}$ until a 50% decrease in load was detected[39,49]. During tensile testing no slippage was noted. Load and crosshead displacement data were recorded at 1500 Hz, and load-deformation and stress-strain curves were generated for

		Injured control tendons (left Achilles) -1-	Injured tendons treated with collagen implant (left Achilles) -2-	Normal tendons -3-	P value 1 vs 2	P value 2 vs 3
		Mean and standard deviation	Mean and standard deviation			
Number of collagen fibrils based on their category and numbers in ultra-micrographs at the same magnification (39000)	Fibrils (0-64 nm) (n)	228.35±17.78	371.36±12.49	56.78±5.39	0.001	0.001
	Fibrils (65-102 nm) (n)	50.85±16.71	91.36±9.53	18.39±2.11	0.001	0.001
	Fibrils (103-153 nm) (n)	0	23.74±12.12	17.68±3.53	0.001	0.592
	Fibrils (154-256 nm) (n)	0	0	22.38±3.88		
	Fibrils (256-307 nm) (n)	0	0	3.34±0.89		
	Total (n)	290.47±41.91	498.62±17.52	118.24±2.85	0.001	0.001
Diameter of collagen fibrils based on their category and numbers in ultra-micrographs (nm)	Fibrils (0-64 nm) (D)	38.17±3.89	51.43±1.33	48.79±2.42	0.001	0.089
	Fibrils (65-102 nm) (D)	70.68±3.5	92.39±4.04	100.45±5.39	0.001	0.111
	Fibrils (103-153 nm) (D)	0	111.86±3.81	149.79±10.89	0.001	0.001
	Fibrils (154-256 nm) (D)	0	0	238.78±4.21		
	Fibrils (256-307 nm) (D)	0	0	276.48±21.33		
	Total (D)	42.45±2.37	61.61±2.77	110.16±9.76	0.001	0.001
Total cross-sectional area of the fibrils/area of the ultra-micrographs	Fibril Density (%)	55.99±4.97	71.73±4.68	89.47±5.59	0.001	0.001
Number of elastic fibers in ultra-micrographs	Elastic Fiber (n)	1.11±0.388	5.29±0.79	9.56±1.29	0.001	0.001
Diameter of the cells and elastic fibers (nm)	Immature Fibroblast (D)	7580.23±260.02	5737.96±330.73	-	0.001	
	Mature Fibroblast (D)	3329.08±282.39	2912.29±169.06	-	0.102	
	Fibrocyte (D)	1560.14±83.83	1313.35±61.09	985.49±54.82	0.022	0.001
	Elastic Fiber (D)	95.98±10.47	207.99±12.48	279.27±14.28	0.001	0.001

Ultra-micrographs: *n=5*. Ultrathin-sections: *n=5*. Tendon samples: *n=10*. Total ultra-micrographs for each group: *n=250*. Independent sample *T-test* was used to compare the significant differences between the left (injured) tendons of the treated and control groups. Paired sample T-test was used to compare the significant differences between the injured treated and intact tendons. Significant differences was determined at confidence interval of *95%* and *P<0.05*. Abbreviations: D=diameter, n=number.

Table 3. Ultrastructural findings in the injured treated, injured control and intact tendons, 120 days post injury and surgical reconstruction (quantitative data from transmission electron microscopy).

each specimen using Test Works 4 software (SUME Systems Corporation). The maximum load, stiffness, maximum stress and modulus of elasticity of the samples were determined.

Statistical analysis

The measured values of injured tendons of each group (left leg) were compared statistically with the measured values of those of their normal contra-lateral tendons (right legs) of the same group at one time point, using paired sample *t-Test*. The measured values of the left tendons of the treated animals were compared with those of the left tendons of the control animals at one time point, using the independent sample *t-Test*. For multiple comparisons the repeated measure and one way ANOVA were used to statistically analyze the differences within and between the groups when appropriate. The quantitative results were expressed as mean ± standard deviation (SD). The correlation between bioelectrical variables and biomechanical variables was performed by ''Pearson's correlation test''. Mann-Whitney *U*-Test was used to analyze the scored values statistically. All statistics were performed using the computer software SPSS version 19 for windows 7 (SPSS Inc. Chicago, IL, USA). Differences of $p<0.05$ were considered significant. The scored data were expressed as median (min-max)[35,36].

Results

Gross pathology

ITTs showed significantly fewer peritendinous adhesions (score 2 (1-3) vs. 3(2-3), *P=0.048*), less hyperemia (score 2 (1-2) vs. 2.5 (2-3), *P=0.046*), and better general appearance (score 2 (0-2) vs. 3 (3-4), *P=0.001*) compared to the ICTs. The diameters of the ITTs in the injured area were significantly greater than those of the ICTs (2.86±0.33 mm vs. 1.75±0.23 mm, *P=0.001*). Generally, the ICTs had adhesions to the surrounding structures and it was difficult to distinguish any demarcation between the regenerated part of the tendon and the peritendinous adhesion. The regenerated tissue was loose,

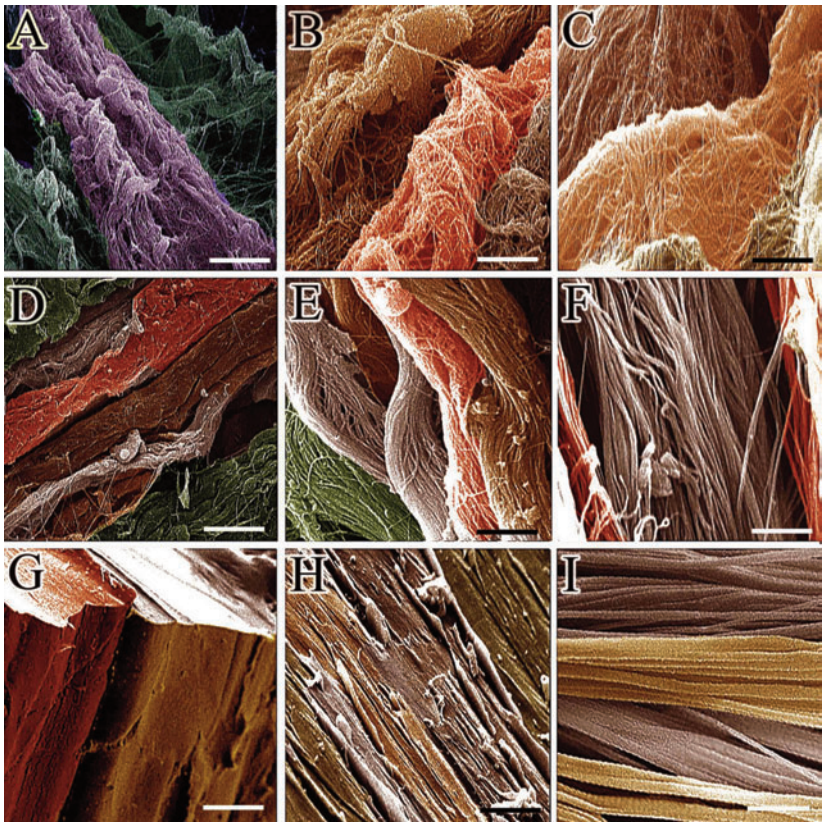

Figure 4. SEM. Injured control tendon (**A-C**). (**A**) No tendinous structure is seen in the injured area and the immature collagen fibrils are the only regenerated nano-structures at this scale (Scale Bar, SB=2 μm). (**B & C**) the newly regenerated collagen fibrils are immature and are lie randomly with no obvious organization and differentiation. No fibres or fibre bundles are seen in the injured area (SB for B and C=1250 and 833nm respectively). (**D-F**) Injured treated tendon. (**D & E**): the collagen structures are highly matured and have been assembled and aggregated so that both fibres (**E**) and fibre bundles (**D**) have formed. The collagen fibrils (**F**) have greater transverse diameter than those in Figure 4C. They are aligned in one direction and they are compact (SB for D-F=2000, 1250 and 833 nm respectively). (**G-I**) Intact tendon: the gross appearance of the tendon (**G**) is so compact that the collagen structural hierarchy could not be differentiated at this magnification (SB=8 μm). In longitudinal section the collagen fibres are highly aligned, ideally organized and compact. No fibrillar components can be identified at this magnification (SB=2500 nm). (**I**) Normal appearance of collagen fibrils in tendon. They are highly aligned and matured. The diameters of these collagen fibrils are larger than those of the collagen fibrils of the injured, treated and untreated tendons (SB=416 nm).

transparent areolar connective tissue (Figure 2A). By contrast the ITTs unlike the ICTs, had a dense, well-organized structure, clearly distinguishable from the surrounding fascia (Figure 2B). These tendons could be dissected and removed easily from the left legs of treated animals. In the ICTs, the severed tendon ends were not covered or filled with the newly regenerated connective tissue (Figure 2A) but in the ITTs, they had completely disappeared and continuity between the ends was fully established (Figure 2B). ITTs showed significantly better scoring for muscle atrophy (2 (1-4) vs. 4 (3-4), *P=0.023*) and muscle fibrosis (2 (0-3) vs. 4 (2-4), *P=0.009*) compared to the ICTs (Figure 2 A-C).

Transmission electron microscopy

Treatment significantly increased number of the newly regenerated collagen fibrils of the ITTs compared to the ICTs at 120 DPI (498.62±17.52 vs. 290.47±41.91, *P=0.001*) so that the ITTs showed more collagen fibrils in the ranges of 0-64 nm (371.36±12.49 vs. 228.35±17.78, *P=0.001*) and 65-102 nm (91.36±9.53 vs. 50.85±16.71, *P=0.001*) compared to the ICTs. Also unlike the ICTs, the ITTs showed some larger collagen fibrils in the range of 103-153 nm (23.74±12.12 vs. 0) in the injured area (Table 3). Treatment also significantly increased the mean total diameter of the collagen fibrils in the ITTs compared to the ICTs (61.61±2.77 nm vs. 42.45±2.37 nm, *P=0.001*) at 120 DPI, so that the diameter of the collagen fibrils in the ranges of 0-64 and 65-102 nm was significantly higher than the ICTs at this stage (*P=0.001, P=0.001*, respectively). Although the mean total diameter of the ITTs was significantly higher than that of the ICTs it was still significantly lower than that of the intact tendons (61.61±2.77 nm vs. 110.16±9.76 nm, *P=0.001*) (Table 3).

Variable (120 DAI)	Unit	Injured control tendons (1) (left)	Injured treated tendons (2) (left)	Normal tendons of the control group (3) (right)	Normal tendons of the treated group (4) (right)	P value (1 vs 2)	P value (2 vs 4)	P value (3 vs 4)
Maximum load	*Newton (N)*	41.42±5.77	118.91±16.07	344.07±39.15	349.32±33.09	0.001	0.001	0.924
Stiffness	*(N)/mm*	11.7±2.01	59.21±5.06	211.79±28.59	203.32±19.31	0.001	0.001	0.838
Maximum stress	*(N)/mm²*	11±1.39	18.54±2.32	32.62±4.05	33.31±3.44	0.001	0.001	0.976
Modulus of elasticity	*(N)/mm²*	0.53±0.1	1.38±0.23	2.99±0.38	3.15±0.46	0.001	0.001	0.898
Dry matter	%	17.75±2.05	30.38±2.22	50.98±2.31	51.19±4.51	0.001	0.001	0.901
Hydroxy proline	µg/mg dry matter	16.73±1.44	41.22±4.75	86.92±7.76	83.28±6.59	0.001	0.001	0.881
Micro-amp	µA	79.16±4.13	42.82±3.61	18.76±6.54	21.39±4.82	0.001	0.001	0.692
Micro-ohm	µΩ	43.15±5.03	72.55±6.19	195.38±22.09	180.51±14.77	0.001	0.001	0.651

Independent sample *T-test* was used to compare the significant differences between the left (injured) legs of the treated groups and control groups. Paired sample T-test was used to compare the significant differences between the injured treated and intact tendons. Significant differences was determined at confidence interval of *95%* and *P<0.05*.

Table 4. Biomechanical, biochemical and bioelectrical characteristics of the injured treated, injured control and their normal contralateral tendons, 120 days after injury and surgical reconstruction (quantitative measurements).

Compared to the ICTs, treatment significantly increased the density of the collagen fibrils at 120 DPI (71.73±4.68 % vs. 55.99±4.97 %, *P=0.001*) but their density was still lower than in the intact tendons (71.73±4.68 % vs. 89.47±5.59%, *P=0.001*). Treatment significantly increased the number and diameter of the elastic fibres and it decreased the transverse diameter of immature tenoblasts and tenocytes compared to those in the ICTs at 120 DPI (*P=0.001, P=0.001, P=0.001, P=0.022* respectively) (Table 3).

The number of tenocytes (measured from 100 cells and reported as percentage) as the most mature mesenchymal cells (Figure 3B and 3C) in the healing area of the ITTs was significantly higher than in the ICTs at 120 DPI (14.97±1.28 % vs. 6.83±1.01 %, *P=0.001*).

Semi-quantitative analysis and descriptive reports of the scanning and transmission electron micrographs

Treatment significantly increased the alignment of the regenerated tissue (2 (2-3) vs. (3 (3-4), *P=0.029*), the maturity of the collagen fibrils (2 (1-3) vs. (4 (3-4), *P=0.003*) and the maturity of the elastic fibres (2 (1-2) vs. (3 (2-3), *P=0.048*) in the ITTs compared to that of the ICTs at 120 DPI (Figure 3 F&G vs. D&E).

The collagen's hierarchical structures were qualitatively more differentiated in the ITTs compared to the ICTs at 120 DPI. At that time unassisted natural healing had not led to formation of large-diameter fibrils or differentiation into hierarchical fibrous architecture (Figure 4 D,E,F vs. A,B,C). However the presence of the collagen prosthesis was associated with well differentiated collagen fibrils and highly matured collagen fibres. Despite this, these latter regenerated fibres were not ultrastructurally identical with those of normal tendon (Figure 4A).

The most characteristic collagenous structures in ICTs were immature, unorganized, low-density collagen fibrils, in multidirectional and disorganised patterns (Figure 3E). Most of the ultra-structural fields from the injured area were filled with unimodal small-sized collagen fibrils lacking any higher tendon architecture such as fibre bundles and fascicles (Figure 3D and Figure 4 A&B). However in ITT tissue, the collagen fibrils were aggregated and arranged in parallel structures to produce highly aligned collagen fibre structures (Figure 4E). These fibres showed bi- or tri-modal distribution patterns consisting of various collagen fibril sizes and were organized in one direction (Figure 3G). At low magnification they could be seen to form fibre bundles (Figure 4D).

Dry matter and hydroxyproline contents

Treatment significantly increased the dry matter content (30.38±2.22 vs. 17.75±2.05, *P=0.001*) and hydroxyproline concentration (as indices of total collagen content) (41.22±4.75 vs. 16.73±1.44 ng/µg dry matter, *P=0.001*) of the ITTs compared to the ICTs at 120 DPI but these value were still significantly lower than their NCTs at this stage (*P=0.001, P=0.001*, respectively) (Table 4).

Biomechanical testing

Treatment significantly increased the maximum load, stiffness, maximum stress and modulus of elasticity of the ITTs compared to the ICTs at 120 DPI (*P=0.001* for all variables). However at this stage, all these values were still significantly lower than their NCTs (*P=0.001* for all variables). There were no significant differences in these variables between the NCTs of the treated and control groups (*P>0.05*) (Table 4).

Amount of PDGF in peripheral blood

Treatment significantly increased the PDGF AA (3.08±0.52 ng/mL vs. 1.04±0.51 ng/mL, *P=0.001*) and PDGF AB (5.04±0.68 ng/mL vs. 2.91±0.63 ng/mL, *P=0.001*) level in the peripheral blood of the treated animals compared to the control

animals. However, these growth factors were still significantly higher in the treated animals compared to the normal level (AA: 3.08±0.52 ng/mL vs. 1.67±0.44 ng/mL, *P=0.001*; AB: 5.04±0.68 ng/mL vs. 0.89±0.28 ng/mL, *P=0.001*).

Bioelectrical characteristics

There were no significant differences between the direct transmission electrical current (micro-amp) of the ITTs and ICTs at 0 DPI (22.24±1.01 μA vs. 22.75±0.82 μA, *P=0.791*). The current in both ITTs and ICTs increased at 7 DPI but that for the ITTs was significantly less than that for the ICTs (110.12±7.98 μA vs.189.72±13 μA, *P=0.001*). The current through the ITTs was significantly less at 120 DPI than that of the ICTs (42.82±3.61 μA vs. 79.16±4.13 μA, *P=0.001*) but these values were significantly higher than their NCTs at this stage (42.82±3.61 μA vs. 22.75±0.82 μA, *P=0.001*).

There were no significant differences between the tissue resistance to direct transmission electrical current (micro-ohm) of the ITTs and ICTs at 0 DPI (185.25±4.74 μΩ vs. 184.05±6.88 μΩ, *P=0.842*). However the resistance of the ITTs was significantly higher than that of the ICTs at 7 DPI (15.05±1.39 μΩ vs. 4.45±0.99 μΩ, *P=0.001*) and remained higher at 120 DPI (72.55±6.19 μΩ vs. 43.15±5.03 μΩ, *P=0.001*). However, the electrical resistance of the ITTs was still significantly lower than that of their NCTs at this stage (72.55±6.19 μΩ vs. 186.11±6.91 μΩ, *P=0.001*) (Table 4).

Correlation tests

There was a negative correlation between the maximum load and micro-amp (r=-0.665, *P=0.036*) and a positive correlation between the maximum load and micro-ohm (r=0.711, *P=0.021*) in the treated tendons. There was also a negative correlation between the stiffness and the micro-amp (r=-0.665, *P=0.036*) in the treated tendons. There was no correlation between the stiffness and micro-ohm of the treated tendons (r=0.326, P=0.161). There was a negative correlation between the maximum load and micro-amp (r=-0.862, *P=0.001*) and a positive correlation between the maximum load and micro-ohm (r=0.694, *P=0.026*) in the control tendons. There was also a negative correlation between the stiffness and the micro-amp (r=-0.878, *P=0.001*) and a positive correlation between the micro-ohm and stiffness (r=0.752, *P=0.012*) in the control tendons. There was also a negative correlation between the micro-amp and micro-ohm of the treated tendons (r=-0.752, *P=0.012*) and also a negative correlation between the micro-amp and micro-ohm of the control tendons (r=-0.452, *P=0.045*). There was no correlation between the micro-ohm and micro-amp with the maximum stress and modulus of elasticity of the treated and control lesions (*P>0.05*).

Discussion

Treatment significantly improved the biomechanical properties of the newly regenerated tissue compared to the control lesions. These beneficial effects indicate that the 3-dimensional collagen implant was able to influence positively the quality of the healing response compared to that of natural healing of large experimental defects in rabbit tendon. The beneficial effect of this treatment strategy may have due to a number of factors or mechanisms such as improved collagen fibrillogenesis, increased diameter and density of the collagen fibrils, more rapid collagen differentiation, earlier development of hierarchical organization, provision of a template for fibril alignment and reduced incidence of peritendinous adhesions. It has been shown that enhanced collagen fibrillogenesis and increases in the diameter of the collagen fibrils play a substantial role in determining collagen density and that these factors can significantly improve the biomechanical properties of a healing tendon[1,35,36,40]. It has also been demonstrated that larger numbers of collagen fibrils and greater diameters of the fibrils confer higher biomechanical performance on healing tendons[1,35,36,39,44].

Parry et al[44] showed that the diameter distributions of the collagen fibrils at birth and in the foetal stages of development are unimodal, whereas at maturity the mass-average diameter of the collagen fibrils is generally larger than at birth and the distributions of fibril sizes may be either unimodal or bimodal depending on the tissue. They showed that both the mean and mass-average diameters of the collagen fibrils are smaller than those at maturity and the fibril distributions are mainly bimodal. They showed that there may be a relation between a bimodal fibril diameter distribution at maturity and the maintenance over long periods of time of either high stress in stretched tissues. The ultimate tensile strength of a connective tissue and the mass-average diameter of the constituent collagen fibrils have been shown to have a positive correlation. In addition, the form of the collagen fibril diameter distribution can be directly related to the mechanical properties of the tissue. If the tissue is primarily designed to have high tensile strength, then an increase in the diameter of the collagen fibrils will parallel an increase in the potential density of intrafibrillar covalent crosslinks. Consequently large collagen fibrils are predicted to have a greater tensile strength than small fibrils.

SEM observations show that this collagen implant not only aggregated the small collagen fibrils into larger ones but that it also improved the hierarchical organization of the healing tendon so that collagen fibrils assembled to form collagen fibres and fibre bundles. Collagen fibrils are the smallest and perhaps the main elements which are responsible for the biomechanical properties of strong, soft connective tissues such as tendons and ligaments[45,46]. Thus, any changes to these structures are likely to change the biomechanical performance of the newly regenerated tissue significantly[44,45].

At a gross pathological level, the collagen implant appeared to be completely absent at 120 DPI in the ITTs. Furthermore, newly-regenerated tendinous tissue with dense consistency and a shiny glistening surface had substituted the collagen implant, suggesting that the later was completely biodegradable and that no remnant of the scaffold remained at 120 DPI. In addition, the ITTs showed few peritendinous adhesions, with little or no muscle atrophy and muscle fibrosis at the gross pathological level. These findings suggest that the collagen implant

acted as a chemotactic factor for peritendinous fibroblasts, possibly attracting and aligning them to its longitudinal axis between the gastrocnemius muscle and calcaneal tuberosity and initiating an accelerated fibroplasia stage of healing inside the collagen implant[39,45,46]. Thus, the injured tendon was possibly able to move in its space relatively early which may have allowed the animals to bear weight on their injured legs and have more physical activity sooner than the untreated animals. It has been shown that enhanced physical activity and weight-bearing capacities in animals used for transected tendon model studies encourages collagen fibrils to align along the line of stress[40]. The ability of the ITT to move in its space soon after injury, may also increase the functionality of the gastrocnemius muscle, so reducing possible muscle atrophy and fibrosis. On the other hand in the ICT, peri-tendinous adhesion was more numerous than in ITT and muscle atrophy and fibrosis were common. Muscle atrophy may have been due to inability of the ICTs to move in their space thus limiting physical activity, whereas muscle fibrosis seems to be related to inability of the healing response to align the direction of proliferating cells[36]. It has been proposed that during natural unassisted tendon healing peritendinous fibroblasts migrate and proliferate in different directions, thus producing peritendinous adhesions[45,47]. Some of these fibroblasts might migrate into the inactive gastrocnemius muscle and proliferate inside it and cause fibrosis, depositing their collagen fibrils among muscle fibres similarly to their behavior in the lesion, which in the longer term results in muscle fibrosis[2,46,47]. The lower collagen density in the lesions of the control tendons may be a result of this mechanism, if some of the healing potential of the tissue is expended on producing muscle fibrosis rather than tendinogenesis.

Although implant remnants were not apparent grossly, microscopic relics of its collagen fibrils were still discernible at the ultrastructural level. Collagen fibrils of normal mature Achilles tendons have never been reported as being larger than 307 nm in transverse diameter while of those identified as likely remnants from the scaffold some were more than 500 nm[1,35]. These results confirm that the implant was biocompatible in the relatively long term (120 DPI) because some of its collagen fibrils were still present but not phagocytized or surrounded by lymphocytes. Collagen sutures are resorbed by phagocytosis[48] so it is likely that the same mechanism is involved in removal of the collagen prosthesis. By this mechanism most of the collagen implant was probably absorbed and substituted with the newly regenerated connective tissue but, to the knowledge of the authors, such long term preservation of xenogenic-derived collagen fibrils in live tissue has not been shown previously. Presence of these collagen fibrils long term after collagen implantation, suggest that these remnants of the scaffolds are accepted as a part of the new tendon. The preserved collagen fibrils possibly acted as a scaffold for the newly regenerated collagen fibrils and aligned them along their long axes or they may have had a role in their aggregation. If this is the mechanism it may explain why the density and diameter of the collagen fibrils was higher in the ITTs compared to the control group. In a comprehensive study on healing of the transacted superficial digital flexor tendon in rabbits, it has been shown that repeated subcutaneous administration of hyaluronic acid was able to preserve old collagen fibrils in an injured area. It has been postulated that such old collagen fibrils may act as a scaffold for aligning the newly regenerated collagen fibrils, and explain the higher ultimate strength of a treated injured area compared to control untreated lesions[49].

Lower electrical current transmission and higher electrical resistance in the regenerated treated tissue, suggest that higher collagen content should be present in the injured area of the ITTs compared to the ICTs. To substantiate this we investigated both dry matter content and the amount of hydroxyproline of the injured tissues and the results were parallel and well supported the bioelectrical results which added to the value of this real time method. The introduction of the collagen implant significantly increased the dry matter content and hydroxyproline as indices of the collagen content in the ITTs, compared to the ICTs[41,50]. It has been shown that increase in the collagen content of regenerated tissue results in decease of its hydration[45,46]. Compared to other tissues, tendon generally has smaller water content and it has been shown that hydration of the intact tendons is in the range of 30 to 50% depending on sex, age and species of the animals[45,50]. The newly regenerated tissues have less collagen and higher water content than the normal healthy tendons. The electrical resistance of the tissue is therefore decreased because the extra water acts as a conductor for electrons[37]. At later stages of tendon healing, the water content of the healing tissue decreases and the collagen content and hierarchical organization of the tissue are improved so that the electrical conductance decreases and the electrical resistance of the tissue gradually increases. The correlation test between the biomechanical and electrical findings indicates that there was a positive correlation between the electrical resistance with maximum load and stiffness of the tissue and there was a negative correlation between the electrical conductance with those of the maximum load, stiffness and electrical resistance of the tissue. These results suggest that the electrical resistance of the tissue is an index of the tissue function and biomechanics.

Based on the recorded results from the treated lesions it can be suggested that number and diameter of the collagen fibrils contribute to collagen density and the collagen density is an index of total collagen content of the tissue. The total collagen content and the tissue alignment seems to be the most important contributing factors in increasing TRDEC. On the other hand, based on the results recorded from the control lesions, it seems the amorphous nature of the healing control lesions together with their lower collagen content and dry matter content and their higher wet weight have strong contribution in decreasing TRDEC.

One of the merits of our tissue-engineered prosthesis is that the implant is eventually almost completely absorbed so that it bestows its characteristics on the new tendon but does not remain a considerable part of it, as is the case with some other prostheses. For example Nishimoto et al[51] found that after using a poly-L-lactic acid as a prosthesis in a ligament defect

model in rabbits, despite excellent biomechanical properties of the repaired area, the implant was not degraded and no new tissue had replaced the scaffold after 16 weeks. Sato et al[52] investigated several different synthetic-based artificial tendons, such as polylactic acid, the mechanical properties of which declined over 26 weeks, but were not replaced by new ligaments. In contrast Gigante et al[53] used a highly aligned bilamellar membrane of type I purified equine collagen in a multi-lamellar conformation to augment a patellar tendon defect model in rabbits and found that the scaffold was incorporated with the native tendon, which correlates with our results. Similarly Enea et al[54] worked on patellar tendon defect in a sheep model and used an experimental protocol similar to ours, but with a different type of collagen implant, and found that it was incorporated into the repaired tissue after 3-6 months.

One of the limitations of this study was that we did not investigate the inflammatory processes in the lesion a few days after tendon injury to investigate how the collagen implant was initially disintegrated and absorbed. However, we were not sure about the efficacy of this novel bioimplant and our goal was to investigate its efficacy on the outcome of the healing of a large tendon defect model in rabbits. Further molecular, biochemical and biomechanical studies in short term observations are needed to explain possible mechanisms by which this implant influences tendon healing. Also variation between the animal studies and human clinical practice should also be considered as one of the potential weaknesses of this study.

Conclusion

Combination of electrospinning technology and randomized gel system a 3-dimentional collagen implant has produced a prosthesis which may be considered as a new option in tendon reconstructive surgery. Our investigation showed the beneficial effects of this implant on the healing of a large tendon defect model in rabbits. The implant increased the biomechanical properties of the newly regenerated tissue compared to the control tendons because it was able to significantly increase fibrillogenesis, enhanced the diameter and density of the collagen fibrils and aligned them along the longitudinal axis of the tendon. This collagen implant also improved the hierarchical organization of the injured area so that the collagen fibrils were assembled to fibres and fibre bundles, and the healed treated tendons were closer to the normal tendons as compared with the control tendons. This treatment regimen also had a role in decreasing the peritendinous adhesion, disuse muscle atrophy and muscle fibrosis. This technology and the newly manufactured collagen implant needs more verification to be applicable in human or veterinary practice, but based on the findings of the present experiment it may be valuable in the near future as one of the options in tendon reconstructive surgery.

Acknowledgements

The authors would like to thank the authorities of Shiraz University and Iranian National Science Foundation (INSF) for their financial support (grant number: 87020247). They are also grateful to Ali Safavi, Mohammad-reza Solhpoor and Ghasem Yousefi from the Departments of Electron Microscopy, Material Sciences and Pathology Department of Shiraz University, for their technical assistance.

References

1. Moshiri A, Oryan A. Structural and functional modulation of early healing of full-thickness superficial digital flexor tendon rupture in rabbits by repeated subcutaneous administration of exogenous human recombinant basic fibroblast growth factor. J Foot Ankle Surg 2011; 50(6):654-62.
2. Chalmers J. Review article: Treatment of Achilles tendon ruptures. J Orthop Res 2000;8(1):97-9.
3. Peterson RK, Shelton WR, Bomboy AL. Allograft versus autograft patellar tendon anterior cruciate ligament reconstruction: A 5-Year Follow-up. Arthroscopy 2001;17(1):9-13.
4. Chen J, Xu J, Wang A, Zheng M. Scaffolds for tendon and ligament repair: review of the efficacy of commercial products. Expert Rev Med Devices 2009;6(1):61-73.
5. Maffulli N, Longo UG, Loppini M. New options in the management of tendinopathy. Open Access J Sports Med 2010;1:29-37.
6. Yang M, Wang Z, Li Y, Guo B. Bilateral cadaveric Achilles tendon graft in reconstruction after tendon tumor resection. J Foot Ankle Surg 2012 Aug 1; in press.
7. Veillette CJ, Cunningham KD, Hart DA, Fritzler MJ, Frank CB. Localization and characterization of porcine patellar tendon xenograft antigens in a rabbit model of medial collateral ligament replacement. Transplantation 1998;65(4):486-93.
8. Allman AJ, McPherson TB, Badylak SF, et al. Xenogeneic extracellular matrix grafts elicit a TH2-restricted immune response. Transplantation 2001;71(11):1631-40.
9. Iannotti JP, Codsi MJ, Kwon YW, et al. Porcine small intestine submucosa augmentation of surgical repair of chronic two tendon rotator cuff tears. A randomized, controlled trial. J Bone Joint Surg Am 2006;88(6):1238-44.
10. Pieper JS, Oosterhof A, Dijkstra PJ, Veerkamp JH, van Kuppevelt TH. Preparation and characterization of porous crosslinked collagenous matrices containing bioavailable chondroitin sulfate. Biomaterials 1999;20(9):847-58.
11. Sahoo S, Cho-Hong JG, Siew-Lok T. Development of hybrid polymer scaffolds for potential applications in ligament and tendon tissue engineering. Biomed Mater 2007; 2(3):169-73.
12. Saeidi N, Guo X, Hutcheon AE, et al. Disorganized collagen scaffold interferes with fibroblast mediated deposition of organized extracellular matrix *in vitro*. Biotechnol Bioeng 2012;109(10):2683-98.
13. Mouquet F, Lemesle G, Delhaye C, et al. The presence of apoptotic bone marrow cells impairs the efficacy of cardiac cell therapy. Cell Transplant 2011;20(7):1087-97.
14. Boland E D, Matthews JA, Pawlowski KJ, et al. Electrospinning collagen and elastin: Preliminary vascular tissue

engineering. Front Biosci 2004;9:1422-32.
15. Foltran I, Foresti E, Parma B, Sabatino P, Roveri N. Novel biologically inspired collagen nanofibres reconstituted by electrospinning method. Macromol Symp 2008; 269:111-8.
16. Heydarkhan-Hagvall S, Schenke-Layland KS, Dhanasopon AP, et al. Three-dimensional electrospun ECM-based hybrid scaffolds for cardiovascular tissue engineering. Biomaterials 2008;29(19):2907-14.
17. Teng SH, Lee EJ, Wang P, Kim HE. Collagen/hydroxyapatite composite nanofibres by electrospinning. Materials Letters 2008;62(17-18):3055-8.
18. McClure MJ, Sell SA, Simpson DG, Bowlin GL. Electrospun Polydioxanone, Elastin, and Collagen Vascular Scaffolds: Uniaxial Cyclic Distension. J Eng Fibre Fabr 2009;4(5):18-25.
19. Togo S, Sato T, Sugiura H, et al. Differentiation of embryonic stem cells into fibroblast-like cells in three dimensional type 1 collagen gel cultures. *In Vitro* Cell Dev Biol Anim 2011;47(2):114-24.
20. Wang YK, Wang YH, Wang CZ, et al. Rigidity of collagen fibrils controls collagen gel-induced down-regulation of focal adhesion complex proteins mediated by alpha2beta1 integrin. J Boil Chem 2003;278(24):21886-92.
21. Xu B, Chow MJ, Zhang Y. Experimental and modeling study of collagen scaffolds with the effects of crosslinking and fibre alignment. Int J Biomater 2001; doi:1155/2011/1723892011.
22. Doillon CJ, Silver FH. Collagen-based wound dressing: effects of hyaluronic acid and fibronectin on wound healing. Biomaterials 1986;7(1):3-8.
23. Postlethwaite AE, Seyer JM, Kang AH. Chemotactic attraction of human fibroblasts to type I, II, and III collagens and collagen-derived peptides. Proc Natl Acad Sci USA 1978;75(2):871-5.
24. Anselme K, Bacques C, Charriere G, et al. Tissue reaction to subcutaneous implantation of a collagen sponge. A histological, ultrastructural, and immunological study. J Biomed Mater Res 1990;24(6):689-703.
25. Liu Y, Ramanath HS, Wang DA. Tendon tissue engineering using scaffold enhancing strategies.Trends Biotechnol 2008;26(4):201-9.
26. Oryan A, Goodship AE, Silver IA. Response of a Collagenase-Induced Tendon Injury to Treatment with a Poly sulphated Glycosaminoglycan (Adequan). Connect Tissue Res 2008;49(5):351-60.
27. Oryan A, Silver IA, Goodship AE. Effects of Serotonin S2-receptor blocker on healing of acute and chronic tendon injuries. J Invest Surg 2009;22(4):246-55.
28. Badylak SF. Xenogeneic extracellular matrix as a scaffold for tissue reconstruction. Transpl Immunol 2004;12:367-77.
29. Yunoki S, Nagai N, Suzuki T, Munekata M. Novel Biomaterial from Reinforced Salmon Collagen Gel Prepared by Fibril Formation and Cross-Linking. J Biosci Bioeng 2004;98(1):40-7.
30. Montanez-Sauri SI, Sung KE, Puccinelli JP, Pehlke C, Beebe DJ. Automation of three dimentional cell culture in arrayed microfluidic devices. J Lab Autom 2011; 16(3):171-85.
31. Whitlock PW, Smith TL, Poehling GG, Shilt JS, Van Dyke M. A naturally derived, cytocompatible, and architecturally optimized scaffold for tendon and ligament regeneration. Biomaterials 2007;28(29):4321-9.
32. Roeder BA, Kokini K, Sturgis JE, Robinson JP, Voytik-Harbin SL. Tensile Mechanical Properties of Three-Dimensional Type I Collagen Extracellular Matrices With Varied Microstructure. J Biomech Eng 2002;124(2):214-23.
33. Greenstein SA, Fry KL, Bhatt J, Hersh PS. Natural history of corneal haze after collagen crosslinking for keratoconus and corneal ectasia: Scheimpflug and biomicroscopic analysis. J Cataract Refract Surg 2010; 36(12):2105-14.
34. McCall AS, Kraft S, Edelhauser HF, et al. mechanisms of corneal tissue cross-linking in response to treatment with topical riboflavin and long-wavelength ultraviolet radiation (UVA). Invest Ophthalmol Vis Sci 2010;51(1):129-38.
35. Oryan A, Moshiri A. A long term study on the role of exogenous human recombinant basic fibroblast growth factor on the superficial digital flexor tendon healing in rabbits. J Musculoskelet Neuronal Interact 2011;11(2):185-95.
36. Oryan A, Moshiri A, Raayat AR. Novel application of theranekron® enhanced the structural and functional performance of the tenotomized tendon in rabbits. Cells Tissues Organs 2012;196(5):442-55.
37. Poltawski L, Watson T. Bioelectricity and microcurrent therapy for tissue healing – a narrative review. Phys Ther Rev 2009;14:104-14.
38. Czarkowska-paczek B, Bartlomiejczyk I, Przybylski J. The serum levels of growth: PDGF, TGF-BETA and VEGF are increased after strenuous physical exercise. J Physiol Pharmacol 2006;57(2):189-97.
39. Oryan A, Moshiri A, Meimandiparizi AH. Short and long terms healing of the experimentally transverse sectioned tendon in rabbits. Sports Med Arthrosc Rehabil Ther Technol 2012; 4, 14.
40. Oryan A, Moshiri A, Meimandiparizi AH, Raayat Jahromi A. Repeated administration of exogenous Sodium-hyaluronate improved tendon healing in an *in vivo* transection model. J Tissue Viability 2012;21(3):88-102.
41. Oryan A, Moshiri A. Recombinant fibroblast growth protein enhances healing ability of experimentally induced tendon injury *in vivo*. J Tissue Eng Regen Med 2012; doi: 10.1002/term.1534.
42. Dowling BA, Dart AJ, Hodgson IR, et al. Superficial digital flexor tendonitis in the horse. Equine Vet J 2000; 32(5):369-78.
43. Reddy GK. Cross-linking in collagen by nonenzymaticglycation increases the matrix stiffness in rabbit achilles tendon. Exp Diabesity Res 2004;5(2):143-53.
44. Parry DA, Barnes GR, Craig AS. A comparison of the size distribution of collagen fibrils in connective tissues as a function of age and a possible relation between fibril

size distribution and mechanical properties. Proc R Soc Lond B Biol Sci 1978;203(1152):305-21.
45. Sharma P, Maffulli N. Tendon Injury and Tendinopathy: Healing and Repair. J Bone Joint Surg Am 2005;87(1): 187-202.
46. Sharma P, Maffulli N. Biology of tendon injury: healing, modeling and remodeling. J. Musculoskelet Neuronal Interact 2006;6(2):181-90.
47. Khanna A, Friel M, Gougoulias N, Longo UG, Maffulli N. Prevention of adhesions in surgery of the flexor tendons of the hand: what is the evidence? Br Med Bull 2009;90(1):85-109.
48. Bartone FF, Shervey PD, Gardner PJ. Long term tissue responces to catgut and collagen sutures. Invest Urol 1976;13(6):390-4.
49. Oryan A, Moshiri A, Meimandiparizi AH. Effects of sodium-hyaluronate and glucosamine-chondroitin sulfate on remodeling stage of tenotomized superficial digital flexor tendon in rabbits: a clinical, histopathological, ultrastructural, and biomechanical study. Connect Tissue Res 2011;52(4):329-39.
50. Oryan A, Silver IA, Goodship AE. Metrenperone enhances collagen turnover and remodeling in the early stages of healing of tendon injury in rabbit. Arch Orthop Trauma Surg 2010;130(12):1451-7.
51. Nishimoto H, Kokubu T, Inui A, Mifune Y, Nishida K, Fujioka H, Yokota K, Hiwa C, Kurosaka M. Ligament regeneration using an absorbable stent-shaped poly-L-lactic acid scaffold in a rabbit model. Int. Orthop 2012; 36:2379-86.
52. Sato M, Maeda M, Kurosawa H, Inoue Y, Yamauchi Y, Iwase H. Reconstruction of rabbit Achilles tendon with three bioabsorbable materials: histological and biomechanical studies. J Orthop Sci 2000;5:256-67.
53. Gigante A, Busilacchi A, Lonzi B, Cecconi S, Manzotti S, Renghini C, Giuliani A, Mattioli-Belmonte M. Purified collagen I oriented membrane for tendon repair: An *ex vivo* morphological study. J Orthop Res 2013; "In Press''. doi: 10.1002/jor.22270.
54. Enea D, Gwynne J, Kew S, Arumugam M, Shepherd J, Brooks R, Ghose S, Best S, Cameron R, Rushton N. Collagen fibre implant for tendon and ligament biological augmentation. *In vivo* study in an ovine model. Knee Surg Sports Traumatol Arthrosc 2012; "In Press''.